**Cell Systems, Volume *6***

## Supplemental Information

# Widespread Rewiring of Genetic Networks upon Cancer Signaling Pathway Activation

**Maximilian Billmann, Varun Chaudhary, Mostafa F. ElMaghraby, Bernd Fischer, and Michael Boutros**

**Table S2: Gene identifier for the 72 query genes used in the study. Related to Figure 1. For the two independent dsRNA sequences used to target those query genes, please see Table S1.**

| FBgn ID | CG ID | Symbol |
|---|---|---|
| FBgn0001324 | CG8491 | kto |
| FBgn0004379 | CG10923 | Klp67A |
| FBgn0010380 | CG12532 | AP-1-2beta |
| FBgn0010379 | CG4006 | Akt1 |
| FBgn0034970 | CG4005 | yki |
| FBgn0052675 | CG32675 | Tango5 |
| FBgn0039907 | CG2041 | lgs |
| FBgn0026598 | CG6193 | Apc2 |
| FBgn0004597 | CG7281 | CycC |
| FBgn0026597 | CG7926 | Axn |
| FBgn0043012 | CG6056 | AP-2sigma |
| FBgn0023423 | CG3412 | slmb |
| FBgn0015589 | CG1451 | Apc |
| FBgn0015391 | CG11397 | glu |
| FBgn0250786 | CG3733 | Chd1 |
| FBgn0005671 | CG17369 | Vha55 |
| FBgn0025830 | CG5859 | IntS8 |
| FBgn0000212 | CG5942 | brm |
| FBgn0024921 | CG7398 | Trn |
| FBgn0030276 | CG1938 | Dlic |
| FBgn0001291 | CG2275 | Jra |
| FBgn0002945 | CG11614 | nkd |
| FBgn0004378 | CG9191 | Klp61F |
| FBgn0003013 | CG7467 | osa |
| FBgn0034964 | CG3173 | IntS1 |
| FBgn0032863 | CG2508 | Cdc23 |
| FBgn0036038 | CG18176 | defl |
| FBgn0031050 | CG12235 | Arp10 |
| FBgn0036141 | CG6210 | wls |
| FBgn0021825 | CG8269 | Dmn |
| FBgn0000117 | CG11579 | arm |
| FBgn0025781 | CG6759 | Cdc16 |
| FBgn0261385 | CG2092 | scra |
| FBgn0000463 | CG3619 | Dl |
| FBgn0085432 | CG34403 | pan |
| FBgn0004647 | CG3936 | N |
| FBgn0001219 | CG4264 | Hsc70-4 |
| FBgn0013749 | CG11027 | Arf102F |
| FBgn0004009 | CG4889 | wg |
| FBgn0053526 | CG33526 | PNUTS |
| FBgn0000499 | CG18361 | dsh |
| FBgn0003371 | CG2621 | sgg |
| FBgn0052654 | CG32654 | Sec16 |
| FBgn0020238 | CG31196 | 14-3-3epsilon |
| FBgn0004390 | CG6721 | RasGAP1 |
| FBgn0003415 | CG9936 | skd |
| FBgn0004859 | CG2125 | ci |
| FBgn0000119 | CG5912 | arr |
| FBgn0261456 | CG11228 | hpo |
| FBgn0014020 | CG8416 | Rho1 |
| FBgn0043900 | CG11518 | pygo |
| FBgn0015618 | CG10572 | Cdk8 |
| FBgn0031030 | CG14217 | Tao |
| FBgn0010315 | CG9096 | CycD |
| FBgn0001218 | CG4147 | Hsc70-3 |
| FBgn0035851 | CG7999 | MED24 |
| FBgn0001085 | CG17697 | fz |
| FBgn0001230 | CG5436 | Hsp68 |
| FBgn0025637 | CG16983 | skpA |
| FBgn0016797 | CG9739 | fz2 |
| FBgn0029709 | CG3564 | CHOp24 |
| FBgn0005386 | CG8887 | ash1 |
| FBgn0034708 | CG5625 | Vps35 |
| FBgn0030093 | CG7055 | dalao |
| FBgn0002022 | CG10449 | Catsup |
| FBgn0000405 | CG3510 | CycB |
| FBgn0026379 | CG5671 | Pten |
| FBgn0037573 | CG7483 | eIF4AIII |
| FBgn0044028 | CG13076 | Notum |
| FBgn0015024 | CG2028 | Cklalpha |
| FBgn0086357 | CG9539 | Sec61alpha |
| FBgn0014411 | CG14804 | Vps26 |

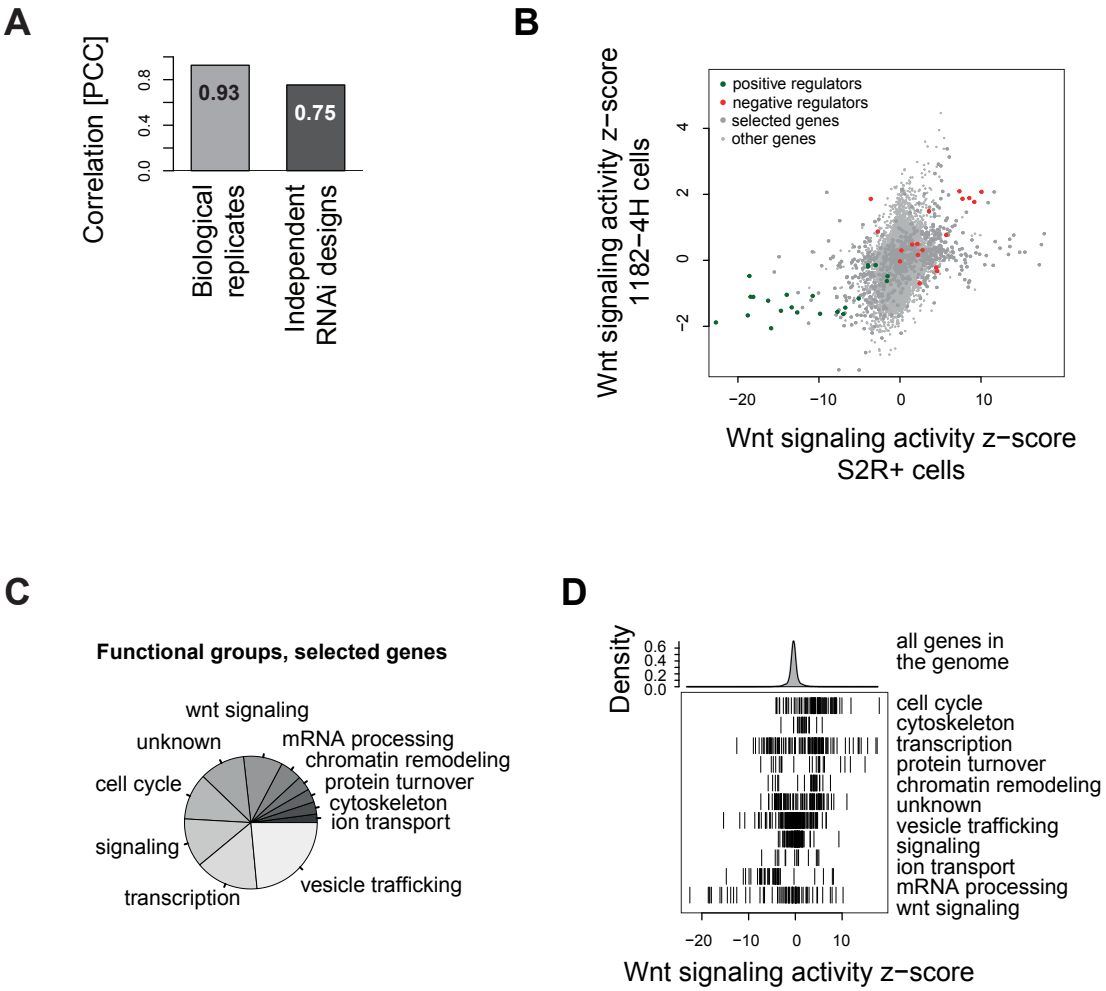
A
Correlation [PCC]
0.0
0.4
0.8
0.93
0.75
Biological replicates
Independent RNAi designs
B
positive regulators
negative regulators
selected genes
other genes
Wnt signaling activity z−score 1182−4H cells
Wnt signaling activity z−score S2R+ cells
C
Functional groups, selected genes
wnt signaling
unknown
mRNA processing
chromatin remodeling
cell cycle
protein turnover
cytoskeleton
ion transport
signaling
vesicle trafficking
transcription
D
Density
all genes in the genome
cell cycle
cytoskeleton
transcription
protein turnover
chromatin remodeling
unknown
vesicle trafficking
signaling
ion transport
mRNA processing
wnt signaling
Wnt signaling activity z−score

**Figure S1**

**Figure S1.** Gene prioritization for genetic interaction analysis in the Wnt signaling pathway. Related to Figure 1. **(A)** Correlation (Pearson correlation coefficient, PCC) of normalized Wnt signaling activity between the biological replicates of the genome-wide RNAi screen, or the two independent dsRNA designs against 13,369 of the 14,331 targeted genes. **(B)** Wnt activity z-scores in *Drosophila* S2R+ and 1182-4H cells. Core Wnt pathway components are highlighted in green (positive regulators) and red (negative regulators). **(C)** Functional groups of the 336 selected genes for Wnt pathway state-dependent quantification of genetic interactions. Genes were assigned to the groups by manual curation. **(D)** Wnt pathway activity z-scores of the selected genes and per functional group as illustrated in (C). Distribution of all dsRNA designs is shown on top for relative comparison.

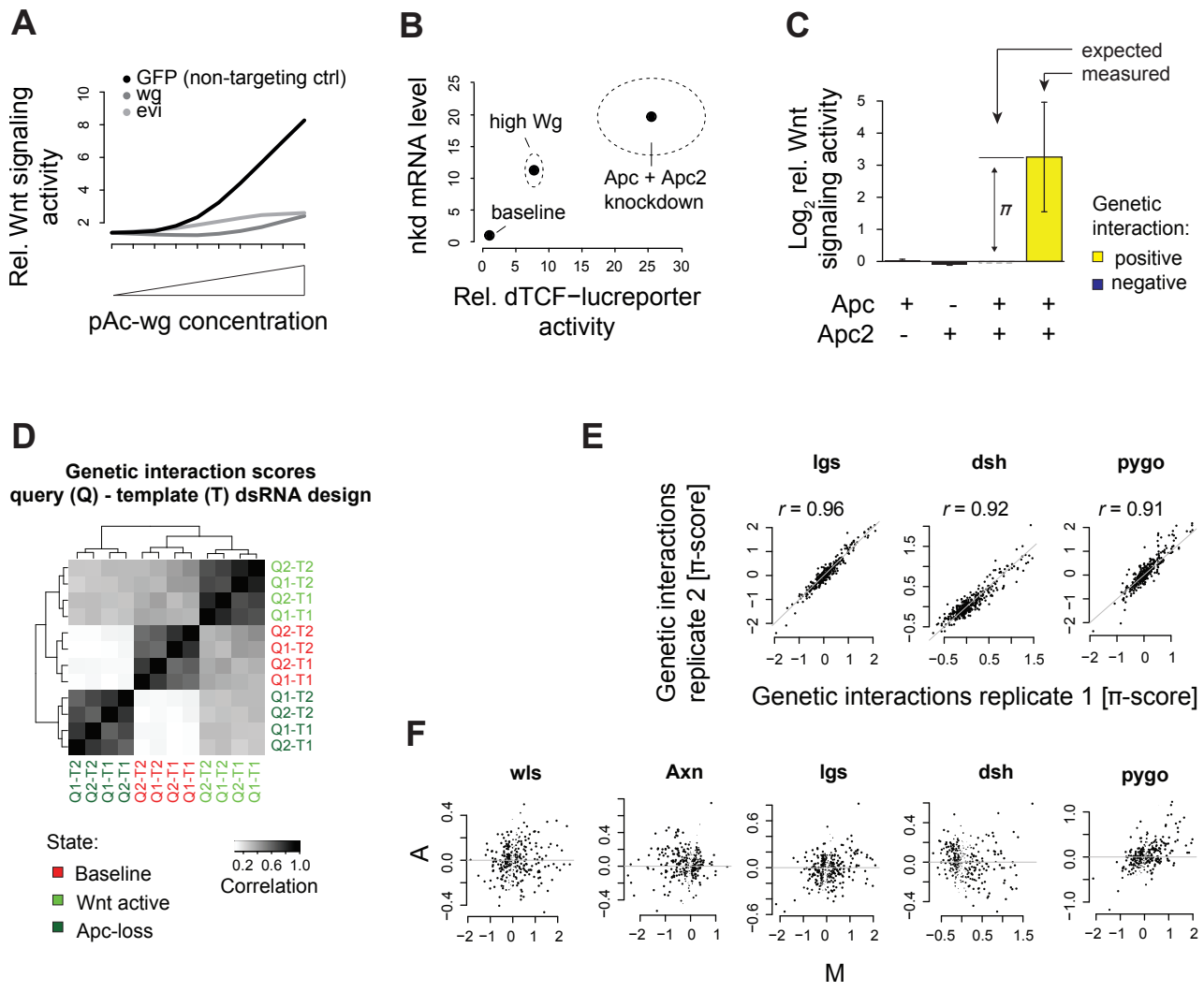
A
GFP (non-targeting ctrl)
wg
evi
Rel. Wnt signaling activity
pAc-wg concentration
B
nkd mRNA level
high Wg
baseline
Apc + Apc2 knockdown
Rel. dTCF−lucreporter activity
C
expected
measured
Log2 rel. Wnt signaling activity
π
Genetic interaction:
positive
negative
Apc
Apc2
D
Genetic interaction scores
query (Q) - template (T) dsRNA design
State:
Baseline
Wnt active
Apc-loss
Correlation
E
lgs
dsh
pygo
r = 0.96
r = 0.92
r = 0.91
Genetic interactions replicate 2 [π-score]
Genetic interactions replicate 1 [π-score]
F
wls
Axn
lgs
dsh
pygo
A
M
G
Pos. genetic interaction
Baseline
Wnt active
Apc-loss
354
110
1352
68
40
431
581
Neg. genetic interaction
Baseline
Wnt active
Apc-loss
383
450
1237
146
37
182
531

**Figure S2**

**Figure S2.** Distinct modes of Wnt pathway activation. Related to Figure 1. **(A)** Fold-change Wnt pathway activity upon increasing concentrations of transfected pAc-wg plasmid. The wildtype pathway activity was measured in 32 wells per concentration and upon transfection of GFP dsRNA (black line). Knockdown of two independent dsRNAs against *wg* and *evi* (*wls*) illustrates that the pathway activity increase was due to Wg expression and secretion (by its cargo receptor Evi). **(B)** Activity levels of the Wnt-specific dTCF-luc reporter and mRNA levels of the Wnt target gene *nkd* in the three pathway states in which we screened for genetic interactions. Wnt reporter activity was measured in 576 wells distributed over six screening batches and *nkd* mRNA levels were quantified by qPCR in biological triplicates. Dashed ellipses illustrate the standard deviation of the data. The data was normalized to the baseline state value. **(C)** Single and combinatorial knockdown phenotypes of *Apc* and *Apc2* illustrating a positive genetic interaction (FDR of 1%). Error bars correspond to the bootstrapped MAD for the single knockdown effects and SD for the combinatorial knockdown measurements. **(D)** Comparison of genetic interaction score replicates within and between states. For each pair of a query (Q) and template (T) gene all four combinations of two independent dsRNA designs were scored independently. Q1-T1 represents the 24120 scores measured between the first query and the first template dsRNA design with the scores measured with the other three Q-T combinations. The Pearson correlation coefficient was used to compare replicates. **(E)** Reproducibility of π-scores with re-screened (four replicates each) query genes *lgs, dsh* and *pygo*, which cover the receptor level and target gene transcription. Pearson correlation coefficients are highly significant ($p < 2.2e-16$). **(F)** M-A-plot showing the deviation A between replicates from their mean M for the five query genes that were re-screened. The size of the dots represents 1 – FDR for each genetic interaction (called for replicate 1). **(G)** Overlap of significant positive (yellow) and negative (blue) genetic interaction (FDR < 1%).

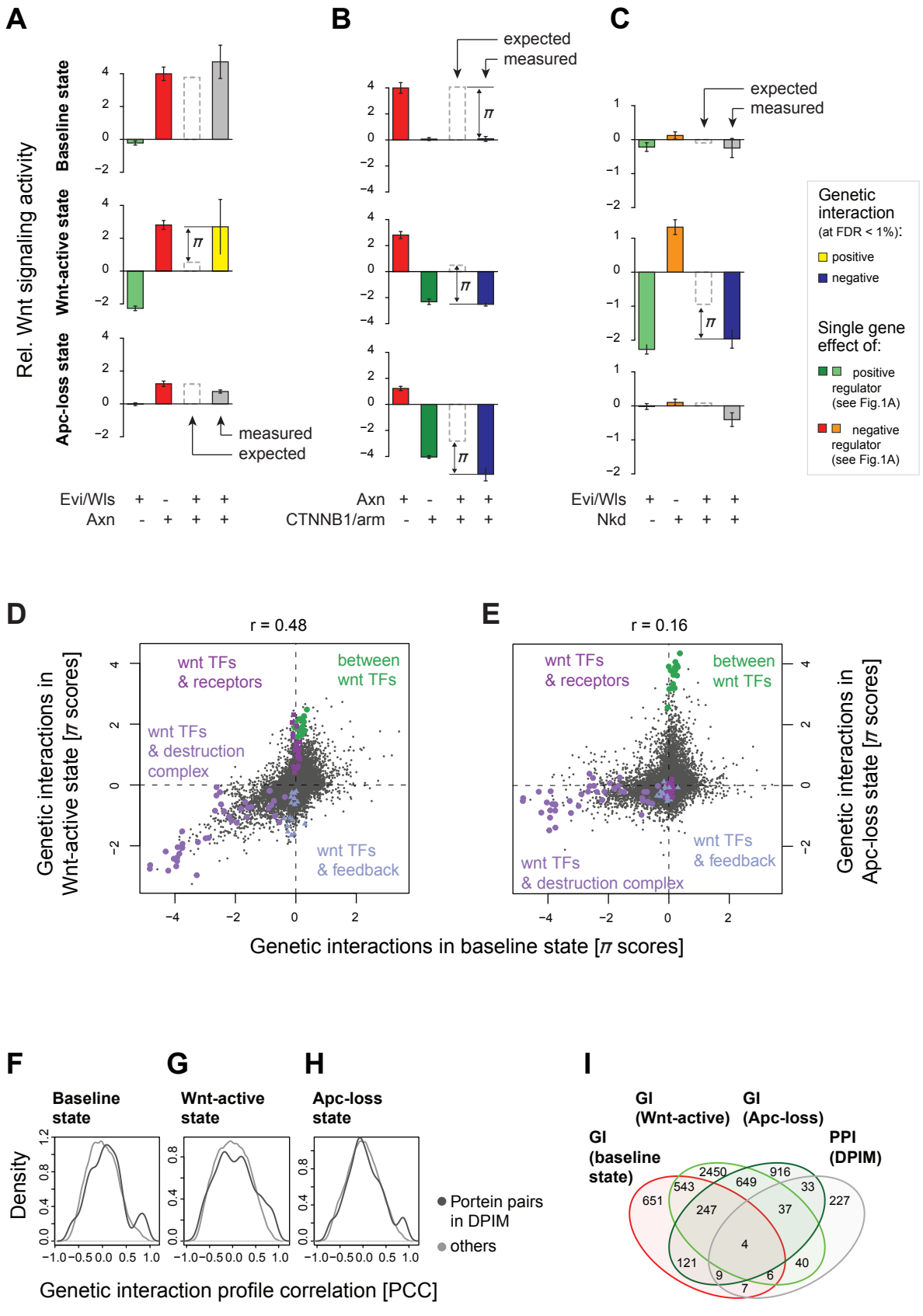
A
B
C
Rel. Wnt signaling activity
Baseline state
Wnt-active state
Apc-loss state
measured
expected
Evi/Wls + - + +
Axn - + + +
Axn + - + +
CTNNB1/arm - + + +
Evi/Wls + - + +
Nkd - + + +
Genetic interaction (at FDR < 1%):
positive
negative
Single gene effect of:
positive regulator (see Fig.1A)
negative regulator (see Fig.1A)
D
E
r = 0.48
r = 0.16
wnt TFs & receptors
between wnt TFs
wnt TFs & destruction complex
wnt TFs & feedback
Genetic interactions in Wnt-active state [π scores]
Genetic interactions in Apc-loss state [π scores]
Genetic interactions in baseline state [π scores]
F
G
H
I
Baseline state
Wnt-active state
Apc-loss state
Density
Portein pairs in DPIM
others
Genetic interaction profile correlation [PCC]
GI (Wnt-active)
GI (Apc-loss)
GI (baseline state)
PPI (DPIM)
651
543
2450
649
916
33
227
247
37
4
121
9
6
40
7

**Figure S3**

**Figure S3.** State-dependent genetic interactions of Wnt signaling. Related to Figure 1. **(A-C)** Combinatorial RNAi enables quantification of genetic interactions representing epistatic relations in the Wnt pathway. Single knockdown phenotypes were estimated from phenotypes of two independent dsRNAs in 144 different genetic backgrounds each (error bars show standard error of median determined by bootstrapping). The white dashed bar indicates the expected combinatorial knockdown effect for each gene pair using a multiplicative neutrality function. The measured combinatorial phenotype illustrates the median of the four possible combinations of two independent dsRNA designs against each gene. The difference between the expected and measured combinatorial phenotype is quantified as a $\pi$-score and quantifies the genetic interaction (yellow if positive, blue if negative at FDR < 1%). The data is presented at $\log_2$ scale. Examples from the Wnt active state are shown in Figure 1C, D. **(D, E)** Complete genetic interactions measured in the baseline state versus ligand-mediated (D) or Apc loss-mediated (G) induction. Genetic interactions between members of known selected functional modules are highlighted. **(F-H)** Comparison of genetic interaction profile correlation and protein-protein interactions. Density of genetic interaction profile correlation of gene pairs that share a protein-protein interaction as reported previously (Guruharsha et al., 2011) (darker line) and those that do not share an interaction in this study (ligher grey line). **(I)** Overlap of significant genetic interactions (FDR 1%) in the baseline, Wnt active and Apc-loss state as well as protein-protein interactions.

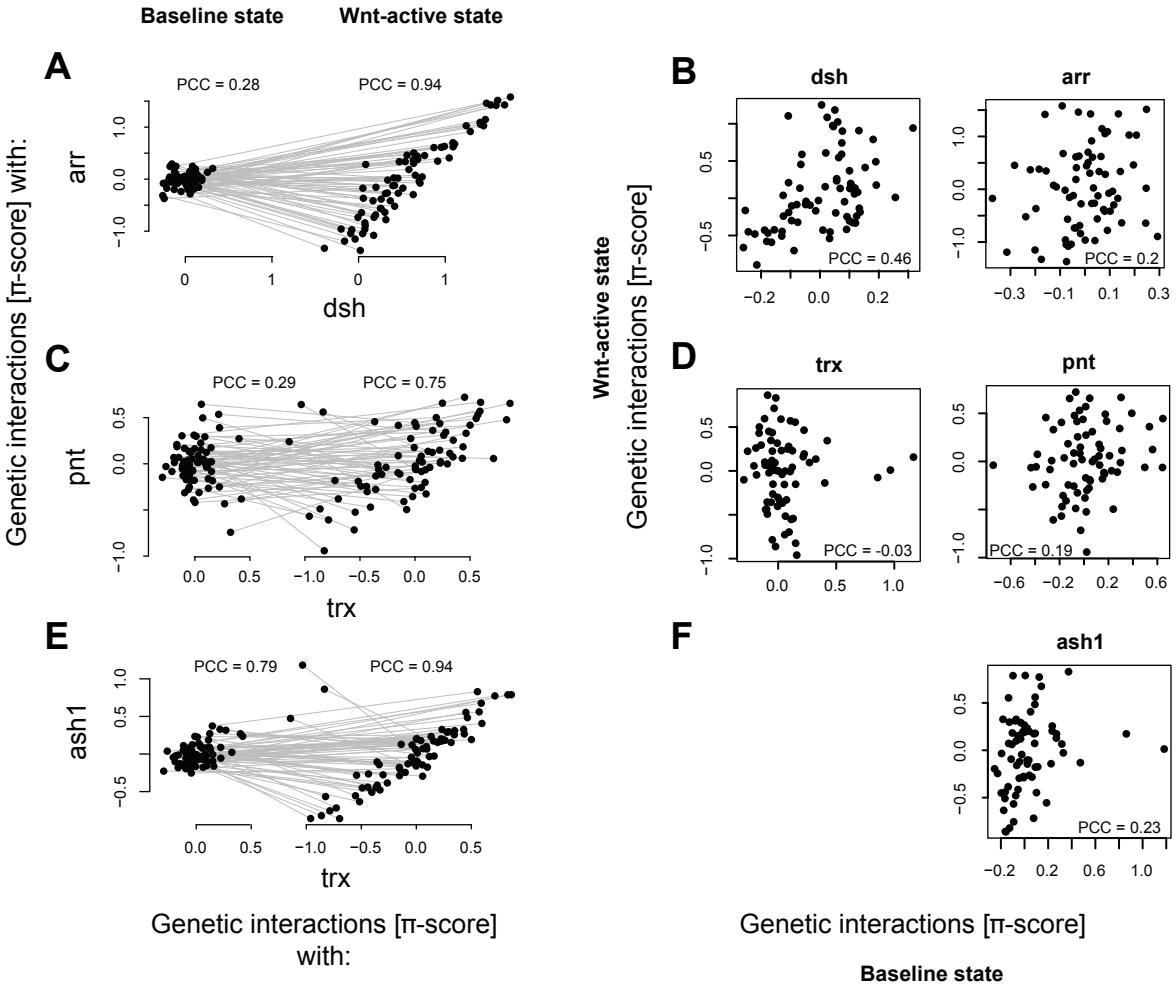
Baseline state
Wnt-active state
A
PCC = 0.28
PCC = 0.94
arr
dsh
B
dsh
arr
PCC = 0.46
PCC = 0.2
C
PCC = 0.29
PCC = 0.75
pnt
trx
D
trx
pnt
PCC = -0.03
PCC = 0.19
E
PCC = 0.79
PCC = 0.94
ash1
trx
F
ash1
PCC = 0.23
Genetic interactions [π-score] with:
Wnt-active state
Genetic interactions [π-score]
Genetic interactions [π-score]
Baseline state

**Figure S4**

**Figure S4.** Genetic interaction profile self-correlation between pathway states and state-specific gene-gene profile correlation. Related to Figure 3. **(A, C, E)** Change of genetic interaction profiles of receptor complex components arr and dsh (A), transcriptional regulators trx and pnt (C) or ash1 (E) from baseline to Wnt-active state. Grey lines connect genetic interaction scores between the gene indicated at the axis and a given query gene. **(B, D, F)** Self-correlation of genetic interaction profiles of the above-mentioned genes between baseline and Wnt-active state.

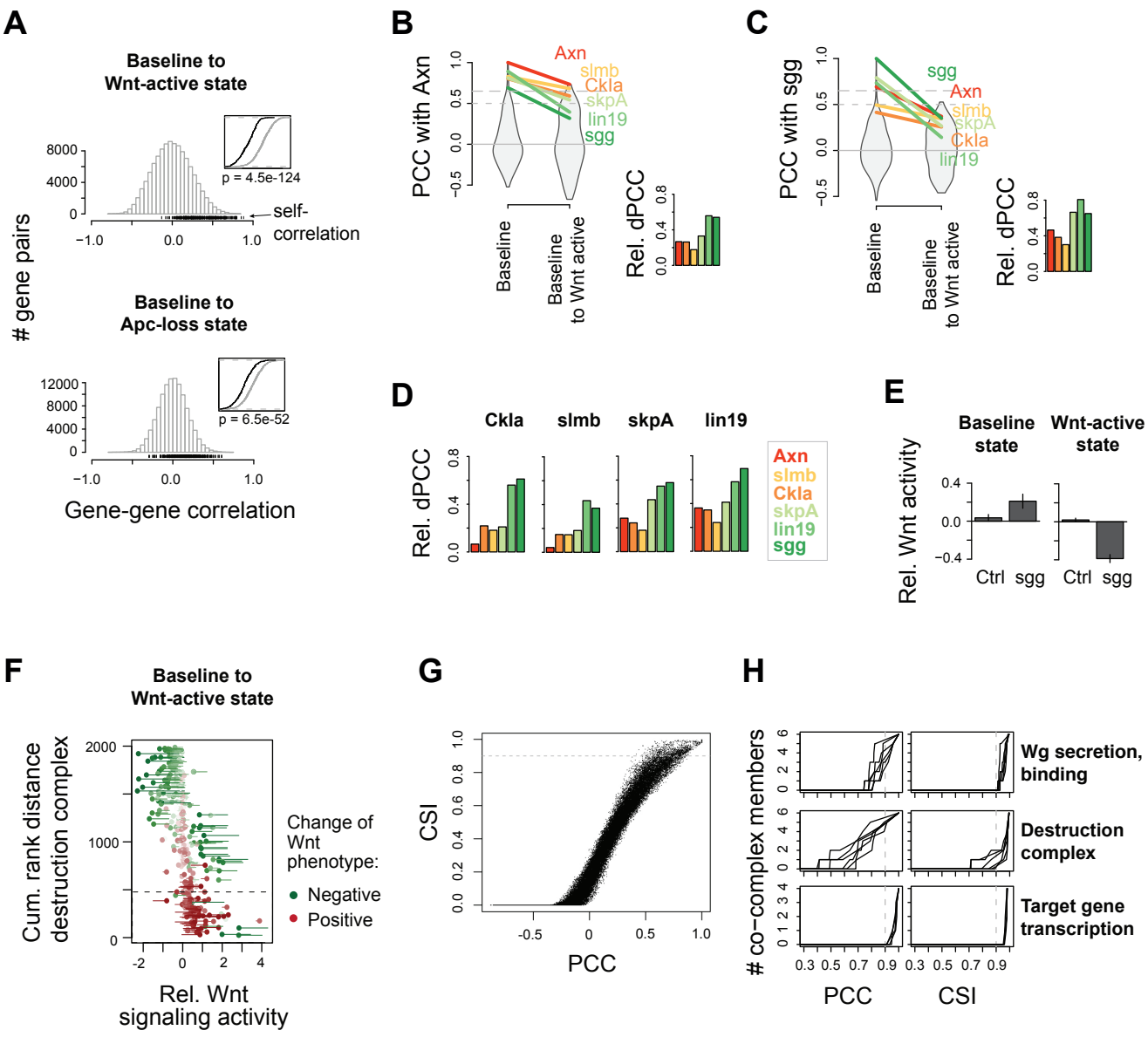
A
Baseline to Wnt-active state
# gene pairs
p = 4.5e-124
self-correlation
Baseline to Apc-loss state
p = 6.5e-52
Gene-gene correlation
B
PCC with Axn
Axn
slmb
Ckla
skpA
lin19
sgg
Baseline
Baseline to Wnt active
Rel. dPCC
C
PCC with sgg
D
Ckla
slmb
skpA
lin19
Rel. dPCC
E
Baseline state
Wnt-active state
Rel. Wnt activity
Ctrl
sgg
F
Baseline to Wnt-active state
Cum. rank distance destruction complex
Change of Wnt phenotype:
Negative
Positive
Rel. Wnt signaling activity
G
CSI
PCC
H
# co−complex members
Wg secretion, binding
Destruction complex
Target gene transcription
PCC
CSI

**Figure S5**

**Figure S5.** Functional plasticity of destruction complex components. Related to Figure 4. **(A)** Distribution of the 112,560 gene-gene between-state relations between baseline and Wnt-active (left) or Apc-loss (right) state. **(B)** Comparison of baseline-specific similarity (Pearson correlation coefficient (PCC) between genetic interaction profiles) with between baseline and Wnt-active state similarity of baseline state Axn with other destruction complex components. The relative differential PCC (Rel. dPCC) shows the slope (baseline-specific PCC minus between-state PCC) relative to the respective baseline-specific PCC. The violin plots show all PCCs with Axn. **(C)** Comparison of baseline-specific similarity with between baseline and Wnt-active state similarity of baseline state sgg with other destruction complex components. **(D)** Relative differential PCC of remaining destruction complex components. **(E)** sgg knockdown effect on Wnt signaling activity in the baseline and Wnt-active state. The single knockdown phenotype was estimated from phenotypes of two independent dsRNAs in 144 different genetic backgrounds each (error bars show standard error of median determined by bootstrapping). **(F)** Change of the single knockdown phenotype upon ligand-mediated pathway activation. Gene depletion lead to more negative (green) or positive (red) pathway activity. The order of genes (y axis) was determined by the between-state cumulative rank distance shown in (Figure 4B). **(G)** Comparison of PCC and CSI illustrating pair-wise similarity in the Wnt active state. The dotted line represents the threshold applied for identifying functional modules in Figure 4D, E. **(H)** Number of members of a given functional module that showed genetic interaction profile similarity with each of the module members when considering the PCC (left) or the CSI (right).

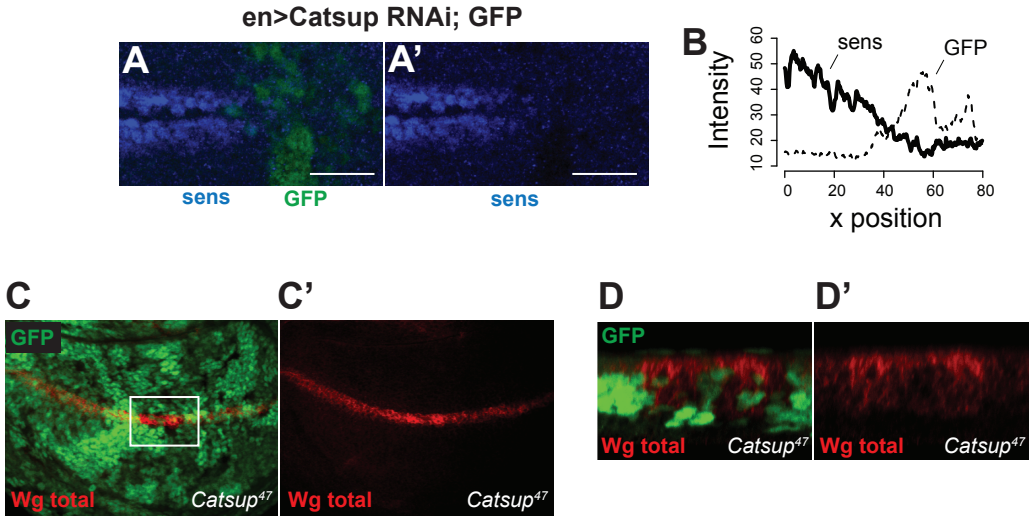
en>Catsup RNAi; GFP
A
A'
sens
GFP
sens
B
Intensity
10 20 30 40 50 60
sens
GFP
0 20 40 60 80
x position
C
C'
D
D'
GFP
Wg total
Catsup47
Wg total
Catsup47
GFP
Wg total
Catsup47
Wg total
Catsup47

**Figure S6**

**Figure S6.** *Catsup* is required for Wg secretion. Related to Figure 5. **(A)** Knockdown of *Catsup* depletes Wnt target gene *sens* expression in the *Drosophila* wing disc. **(B)** Quantification of *sens* expression along the A/P axis of the wing disc. enGal4/UAS-*Catsup*RNAi, posterior to the right. *sens* staining intensity was quantified using FIJI ($n > 4$ wing discs). **(C)** Knockout of *Catsup* in the *Drosophila* wing disc leads to Wg accumulation in the Wg producing cells. **(D)** Wg accumulates at the apical side of the Wg secreting cells in the wing disc. This cross section was reconstructed using z-stacks. $Catsup^{47}$ clones in the *Drosophila* wing disc are marked by the absence of GFP expression.